Journal of Alloys and Compounds 509 (2011) 8927–8932

Contents lists available at ScienceDirect

Journal of Alloys and Compounds

journal homepage: www.elsevier.com/locate/jallcom

Sol–gel assisted preparation and characterization of silver indium diselenide powders

Szu-Chia Chien, Fu-Shan Chen, Chung-Hsin Lu*

Department of Chemical Engineering, National Taiwan University, Taipei, Taiwan, ROC

ARTICLE INFO

Article history:
Received 19 October 2010
Received in revised form 14 June 2011
Accepted 16 June 2011
Available online 22 June 2011

Keywords:
Chalcopyrite
$AgInSe_2$
Sol–gel

ABSTRACT

$AgInSe_2$ powders were successfully prepared via mixing sol–gel derived precursors, followed by a selenization process. To obtain the pure $AgInSe_2$ compound, excess amounts of In^{3+} ions were added into the starting solution to compensate the loss of In_2O_3 during the selenization process. A figure that depicts the relationship between the resultant compounds and different selenization temperatures was constructed according to the formed phases. The Raman spectrum and Rietveld refinement confirmed that the prepared $AgInSe_2$ belonged to the chalcopyrite structure. With increasing selenization temperatures, the $AgInSe_2$ powder particle sizes as well as the crystallinity increased significantly. The $AgInSe_2$ formation mechanism during the selenization process is proposed as a two-step process. Ag_2Se is formed in the first step and then induces the second-step reaction to produce $AgInSe_2$. The sol–gel route with a selenization process is introduced as a new approach to fabricate pure $AgInSe_2$ powders for use in thin-film solar cells.

1. Introduction

Thin-film solar cells have been developed as second generation solar cells with the advantages of low manufacturing cost and efficient material utilization [1]. I–III–IV$_2$ chalcopyrite compounds have the potential for use as the absorber material in thin-film solar cells due to the direct band gap and the high optical absorption coefficient [2–4]. Additionally, I–III–IV$_2$ chalcopyrite compounds can be formed with n or p type [5]. $AgInSe_2$, which has a chalcopyrite structure with a band gap energy of 1.2 eV, serves as a promising candidate for the absorbers in solar cells [6,7]. With the wide band gap characteristic, $AgInSe_2$ can be used as the top cells in tandem solar cells [5].

Various physical and chemical deposition techniques have been developed to prepare the chalcopyrite compounds used in thin-film solar cells, such as the flash evaporation process [8], the thermal evaporation [9], the electron-beam method [10], the sputter deposition [11], and the pulsed laser deposition [12]. The high cost for the vacuum system and intricate processes restrain the popularity of thin-film solar cells. Besides, the common problem encountered during the processes is to preserve a stoichiometric amount of Se due to high volatility in Se-containing compounds. To solve these problems and simplify the process, a non-vacuum ink printing process using particles was developed for preparing solar cell absorbers by different groups [13,14]. The ink printing method has the advantages of low cost and simplified steps. Hence, the synthesis of $AgInSe_2$ powders becomes an important subject. To prepare $AgInSe_2$ powders for ink printing, various routes are developed including the solid-state reaction [15], the hydrothermal method [16] and the one-pot process [17]. These methods provide different approaches to control the sizes, the composition, and morphology of $AgInSe_2$ particles. These reported processes usually require a long reaction duration or complicated synthesis procedures.

To overcome the drawbacks mentioned above, the sol–gel process was employed to synthesize $AgInSe_2$ powders in this study. In the sol–gel process, chelating agents and polymering agents can form a chelation complex which can avoid precipitation and the segregation of metal ions. This results in composition control and excellent homogeneity advantages [18,19]. The $AgInSe_2$ precursors were derived via the sol–gel process with a subsequent heat treatment to remove the organic residuals. $AgInSe_2$ was obtained via mixing the prepared precursors and Se powders, followed by a selenization process. The influence of the ratios of In^{3+} ions to Ag^+ ions in the sol–gel route upon $AgInSe_2$ formation was investigated. The effects of the selenization temperature and duration effects on the $AgInSe_2$ purity were examined. The relation between the selenization conditions and characteristics of the obtained compounds was studied. The reaction mechanism of $AgInSe_2$ formation was also proposed.

---

* Corresponding author. Tel.: +886 2 23651428; fax: +886 2 23623040.
E-mail address: chlu@ntu.edu.tw (C.-H. Lu).

0925-8388/$ – see front matter © 2011 Elsevier B.V. All rights reserved.
doi:10.1016/j.jallcom.2011.06.069

2. Experimental

$AgInSe_2$ powders were synthesized via the sol–gel route employing citric acid and ethylene glycol as the chelating and polymerizing agents, respectively. Indium nitrate ($In(NO_3)_3$) and silver nitrate ($AgNO_3$) were first dissolved in deionized water. The $In(NO_3)_3$ to $AgNO_3$ molar ratios were varied from 1:1 to 1.5:1. Citric acid was then added into the prepared solution one time. The molar ratio of cations (Ag^{3+} and In^{3+} ions) to citric acid was fixed at 1:2. The mixed solution was stirred for 2 h, followed by adding ethylene glycol into the solution one time. The citric acid to ethylene glycol molar ratio was fixed at 1:1.5. The prepared solution was stirred for 6 h and then heated at 300 °C to remove the water and initiate the gelation reaction. During the gelation process, the clear solution turned into a brownish gel. The gel was further heated at 500 °C in air for 3 h to remove the organic residuals. After the heat treatment, the precursor powders containing silver and indium ions were obtained. The obtained precursors were then mixed with excess Se powders and selenized in the reducing atmosphere (5 vol% H_2 and 95 vol% N_2) at 250–600 °C for 20 min to 3 h in a horizontal tube furnace. The molar ratio of cation (Ag^{3+} and In^{3+} ions) to Se powders was fixed at 1:2.5. Once Se powders were heated, the selenium gas was formed and carried by the carrier gas (H_2 and N_2) to induce the senenization reactions.

The formed phases of the prepared powders were examined via an X-ray diffractometer (XRD, Philips X'Pert/PMD) using Cu Kα radiation at 45 kV and 40 mA. The morphology of the obtained $AgInSe_2$ powders was observed using a scanning electron microscope (SEM, Hitachi S-800). The program PDXL Rietveld analysis was used to examine the lattice parameters. A Raman spectrometer (Jobin Yvon (T64000) micro-Raman spectrometer) with an Ar ion laser (λ = 514.5 nm) was performed as a light excitation source.

3. Results and discussion

3.1. Selenization conditions and compositional ratio effects on $AgInSe_2$ powder formation

The $AgInSe_2$ precursors were first prepared via the sol–gel route with an In^{3+}/Ag^{+} ion ratio of 1. After removing the organic residuals, the precursors were then mixed with Se powders, followed by a selenization process. Fig. 1 illustrates the X-ray diffraction patterns of $AgInSe_2$ precursors and powders obtained after selenization at different temperatures ranging from 300 °C to 550 °C. As shown in Fig. 1(a), the precursors were identified as a mixture of Ag and In_2O_3 powders. When the selenization temperature was set at 300 °C (Fig. 1(b)), $AgInSe_2$ with low crystallinity started to form. It is also noted that Ag_2Se, In_2O_3 and Se impurities coexisted with $AgInSe_2$. When selenizing at 400 °C (Fig. 1(c)), the peak intensity of $AgInSe_2$ increased with decreasing peak intensities of impurities (Ag_2Se, Se and In_2O_3). As the selenization temperature was further increased, the crystallinity of $AgInSe_2$ improved. Once the selenization temperature was elevated to 500 °C (Fig. 1(d)), the impurities (Ag_2Se and In_2O_3) remained and Se disappeared. After selenizing at 550 °C (Fig. 1(e)), a large amount of $AgInSe_2$ was formed, however, Ag_2Se still existed in the samples. According to the above results, the pure $AgInSe_2$ phase could not be obtained by varying the selenization temperatures.

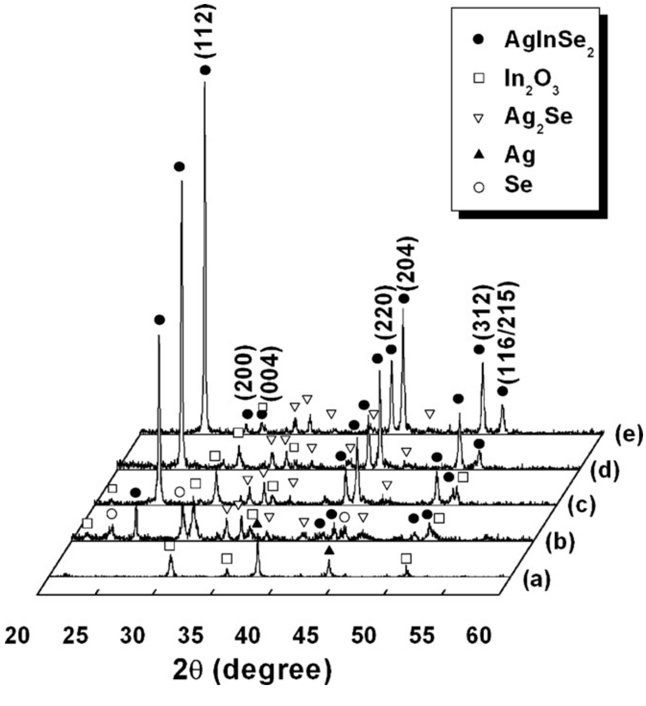

Fig. 1. X-ray diffraction patterns of $AgInSe_2$ precursors (a) and the precursors selenized at (b) 300 °C, (c) 400 °C, (d) 500 °C, and (e) 550 °C for 0.5 h.

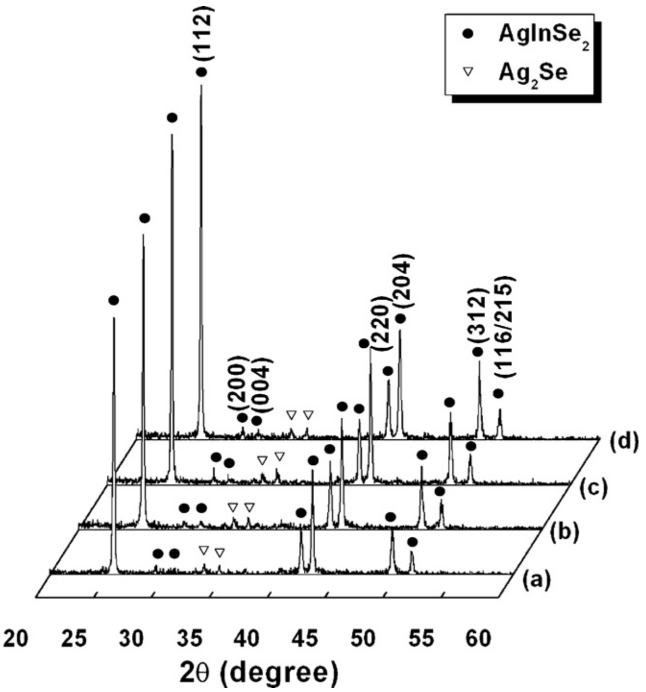

Fig. 2. X-ray diffraction patterns of $AgInSe_2$ selenized at 550 °C for (a) 0.5 h, (b) 1 h, (c) 1.5 h, and (d) 3 h.

The duration of the selenization process was varied to improve the $AgInSe_2$ phase purity. Fig. 2 illustrates the X-ray diffraction patterns of samples selenized at 550 °C for different durations. The diffraction peak intensities of $AgInSe_2$ were observed to increase gradually with the prolonged heating duration from 0.5 h to 3 h. However, the Ag_2Se impurity still coexisted with $AgInSe_2$. Therefore, prolonging the selenization duration could not eliminate the Ag_2Se impurity.

In order to prepare monophasic $AgInSe_2$, In^{3+}/Ag^{+} molar ratios were adjusted from 1 to 1.5. Fig. 3 shows the X-ray diffraction patterns of samples selenized at 550 °C for 0.5 h with various In^{3+}/Ag^{+} molar ratios. As the In^{3+}/Ag^{+} molar ratio was changed from 1 to 1.1 (Fig. 3(a) and (b)), there was no significant change in the formed phases. When the In^{3+}/Ag^{+} molar ratio was set to 1.3 (Fig. 3(c)), the pure phase of $AgInSe_2$ powders was successfully obtained. All peaks in the X-ray patterns were assigned to $AgInSe_2$ with a tetragonal structure as reported in ICDD file No. 75-0118. With the In^{3+}/Ag^{+} molar ratio fixed at 1.5 (Fig. 3(d)), the In_2O_3 impurity was found to coexist with $AgInSe_2$. The above results indicated that it was necessary to add excess In^{3+} ions into the sol–gel solution to obtain pure phase $AgInSe_2$. During the selenization process, the carrier gas was a mixture of 5% H_2/95% N_2 which provided the reducing atmosphere. It has been shown that In_2O_3 will be reduced to indium metal in the reducing atmosphere [20,21]. Since indium metal has a low melting point (156.6 °C), indium metal will vaporize during the selenization process, causing indium species loss. To compensate

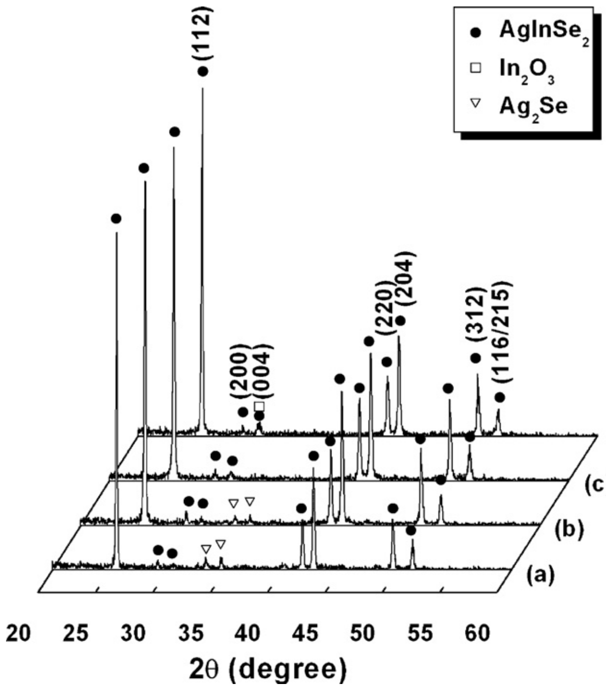

Fig. 3. X-ray diffraction patterns of AgInSe$_2$ powders selenized at 550 °C for 0.5 h with the In^{3+} to Ag$^+$ ratios equal to (a) 1.0, (b) 1.1, (c) 1.3, and (d) 1.5.

the loss of indium species, excess In^{3+} ions are required to produce pure phase AgInSe$_2$. In the developed sol–gel method, the required temperature for synthesizing pure AgInSe$_2$ was 450 °C. On the other hand, the heating temperature of 800 °C is necessary for preparing pure AgInSe$_2$ in the conventional solid-state process [22]. Due to polymerization in the sol–gel solution, tiny gel cages were formed to trap the metal ions, resulting in good homogeneity and small precursor sizes. Hence, the precursor reactivity was improved. The enhanced reactivity can lower the preparation temperatures for pure-phased AgInSe$_2$ powders.

3.2. *Characterization of the prepared AgInSe$_2$ powders*

According to the obtained results, the In^{3+}/Ag$^+$ ion ratio was fixed at 1.3 in the following experiments. AgInSe$_2$ precursors were selenized at different conditions to identify the proper conditions for obtaining the pure phase. The relation between the resultant compounds and different selenization conditions is depicted in Fig. 4. In accordance with the formed phases, the figure can be divided into four zones. In zone I, Ag$_2$Se is formed under comparatively low temperatures and short duration. Ag$_2$Se, In$_2$O$_3$ and Se appear as the main phases in this region. As the selenization temperature is increased to 300 °C and the duration is longer than 20 min, the AgInSe$_2$ phase is formed in zone II. In this region, the Ag$_2$Se, In$_2$O$_3$ and Se impurities still coexist with AgInSe$_2$. In zone III, by increasing the temperature and prolonging the duration, the Se phase disappears. The resultant compounds found in zone III indicate that the Se powders have reacted to form AgInSe$_2$ and Ag$_2$Se. As the selenization temperature is further elevated or the duration is further prolonged, the pure AgInSe$_2$ phase is obtained as shown in zone IV. Fig. 4 reveals that prolonging the duration at low temperature or raising the temperature for a short duration could lead to form the pure AgInSe$_2$ phase.

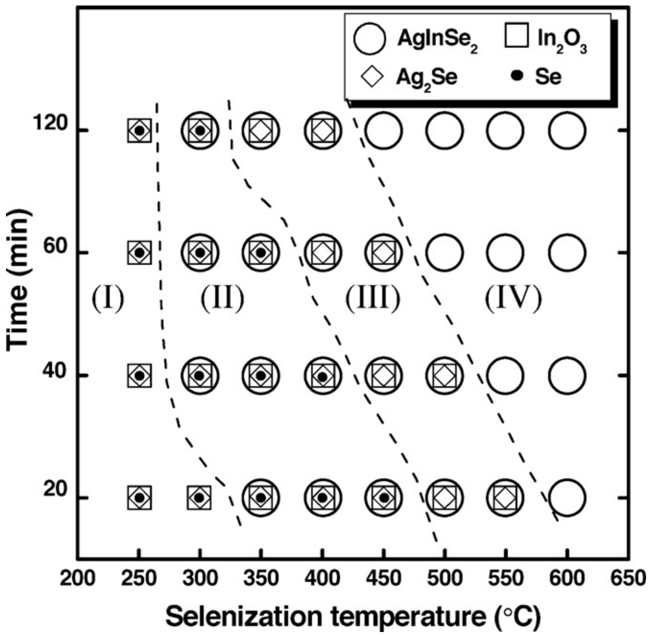

Fig. 4. Resultant compounds of AgInSe$_2$ precursors selenized in different heating conditions.

The Rietveld refinement was used to analyze the obtained AgInSe$_2$ powders. Fig. 5 illustrates the plot of observed and calculated X-ray diffraction patterns with deviation profiles for pure AgInSe$_2$ powders prepared at 550 °C for 0.5 h. Fig. 5 also shows the positions of all reflections with marked vertical bars. The reliability factors, R_p and R_{wp}, were converged by the Rietveld refinement to 3.7% and 4.91%, respectively. Based on the small reliability factors, the refinement results provide a reliable simulation for the prepared AgInSe$_2$ structure. The Rietveld refinement results for AgInSe$_2$ are summarized in Table 1. The lattice parameters, a and c, were calculated to be 6.112 Å and 11.705 Å, respectively. The calculated results from the Rietveld refinement show little compressive distortion of the tetragonal structure as the lattice parameter ratio ($\eta = c/2a$) is smaller than 1. The obtained results were consistent with the literature [23]. The values for *a* and *c*, of AgInSe$_2$

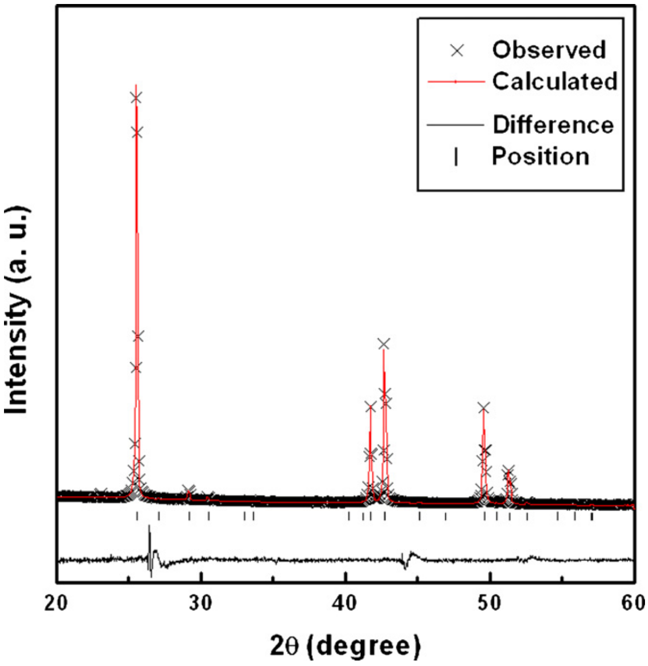

Fig. 5. Observed (×) and calculate (upper solid line) X-ray diffraction pattern of AgInSe$_2$ powders with difference profile (lower solid line) and positions of all the reflections (vertical bars).

Table 1
Rietveld refinement calculations of $AgInSe_2$.

Formula	$AgInSe_2$
Crystal system	Tetragonal
Space group	I-42d
Lattice constants	
a (Å)	6.112
c (Å)	11.705
$\eta = c/2a$	0.9575
Cell volume (Å^3)	437.253
R values	$R_{wp} = 4.91\%$ $R_p = 3.70\%$

were found to be larger than the lattice parameters for $CuInSe_2$ as reported. The differences in the *a* and *c* values result from the greater Ag atom size than the Cu atom, thereby enlarging the distance between the ions in the chalcopyrite structure.

The microstructures of the prepared $AgInSe_2$ at various temperatures for 1 h are shown in Fig. 6. The morphology of the samples obtained at various selenization temperatures was similar. When the selenization temperature was at 350 °C (Fig. 6(a)), the particle morphology exhibited irregular shapes with an average size of 1 μm. The sizes of the large particles were found to increase gradually with the increase in selenization temperature as shown in Fig. 6(b). As the selenization temperatures were further increased to 550 °C (Fig. 6(c)) and 600 °C (Fig. 6(d)), the micrographs show that the average sizes of the powder particles reached 2 μm.

The Raman spectrum of the prepared $AgInSe_2$ selenized at 550 °C for 0.5 h is shown in Fig. 7. The Raman peaks were observed at 141.46 and 164.13 cm^{-1}. The Raman spectrum of the prepared $AgInSe_2$ was similar to the $AgInSe_2$ spectrum reported in the literature [15]. Two major peaks were observed around 141.46 cm^{-1} and 164.13 cm^{-1}, which were assigned B_2 mode and A_1 mode, respectively. The A_1 mode at 164.13 cm^{-1} corresponds to the movement of anions (Se) with other cations at rest in the chalcopyrite structure [24]. The B_2 mode at 141.46 cm^{-1} represents the associated motion between anions (Se) and cations (Ag and In) in the chalcopyrite structure [24]. The above results confirmed the crystal structure of $AgInSe_2$.

3.3. Formation mechanism of $AgInSe_2$

The precursors were selenized to the designed temperatures and then cooled quickly for investigating the $AgInSe_2$ reaction mechanism in the selenization process. As shown in Fig. 8, when selenizing at 300 °C, the main phases were found to be Ag_2Se, In_2O_3 and Se without the existence of Ag (Fig. 8(a)). After selenizing at 400 °C, small amounts of $AgInSe_2$ began to be formed. How-

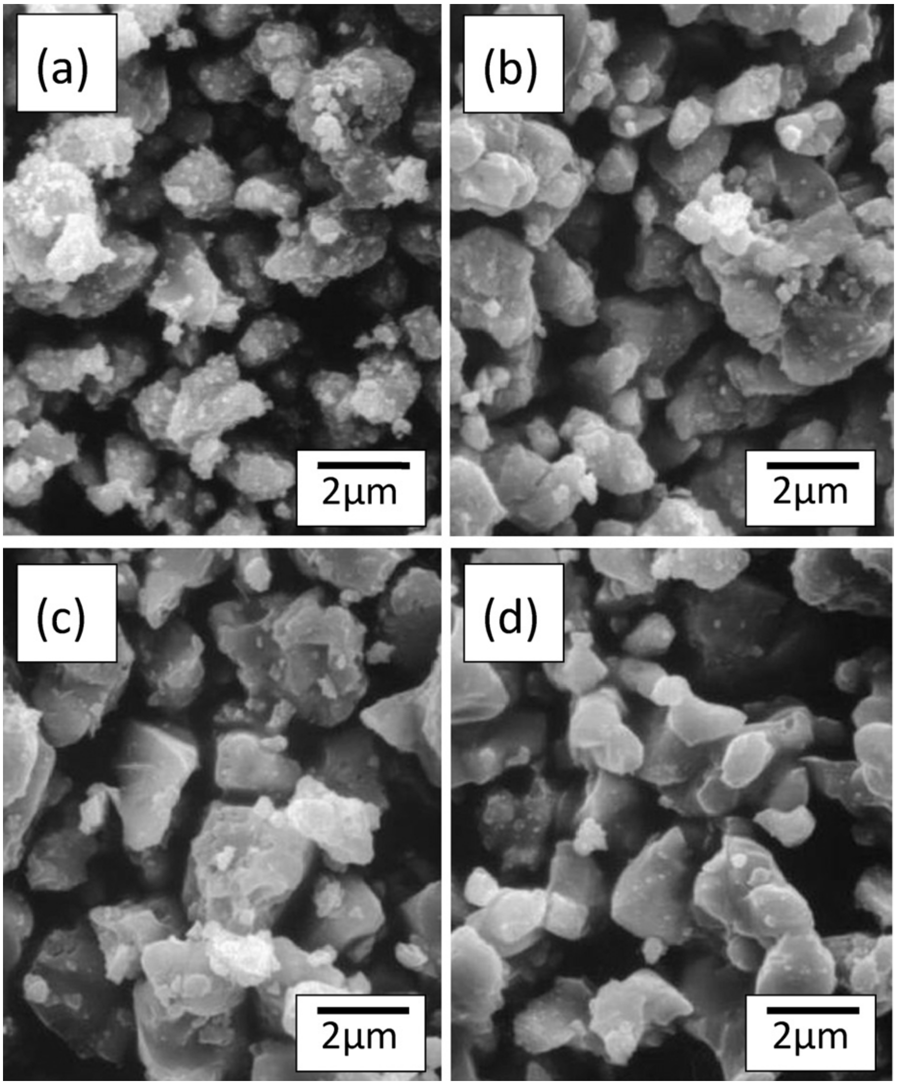

Fig. 6. SEM micrographs of $AgInSe_2$ powders selenized at (a) 350 °C, (b) 450 °C, (c) 550 °C, and (d) 600 °C for 1 h.

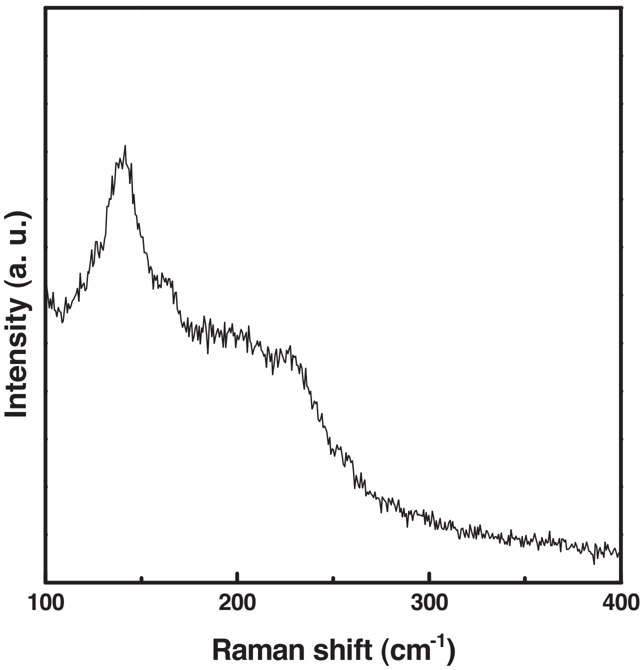

Fig. 7. Raman spectrum of $AgInSe_2$ powders.

ever, large amounts of impurities-Ag_2Se, In_2O_3 and Se still existed (Fig. 8(b)). As the temperature was raised to 500 °C, $AgInSe_2$ became the major phase and small amounts of Ag_2Se and In_2O_3 existed in the prepared powders (Fig. 8(c)). After selenization at 600 °C, the amount of $AgInSe_2$ increased with a decrease in the amounts of Ag_2Se and In_2O_3.

The relation between the X-ray diffraction intensities of the resulting compounds and the selenization temperatures is depicted in Fig. 9. It can be seen that the amounts of Ag and Se diminished at 300 °C and 400 °C, respectively. The amounts of In_2O_3 and Ag_2Se increased slightly at 300 °C, and decreased gradually as the temperature was further raised. $AgInSe_2$ started to appear at 400 °C, and its amount increased as the temperature was elevated. According to the observed results, the supposed reaction schemes are expressed as below:

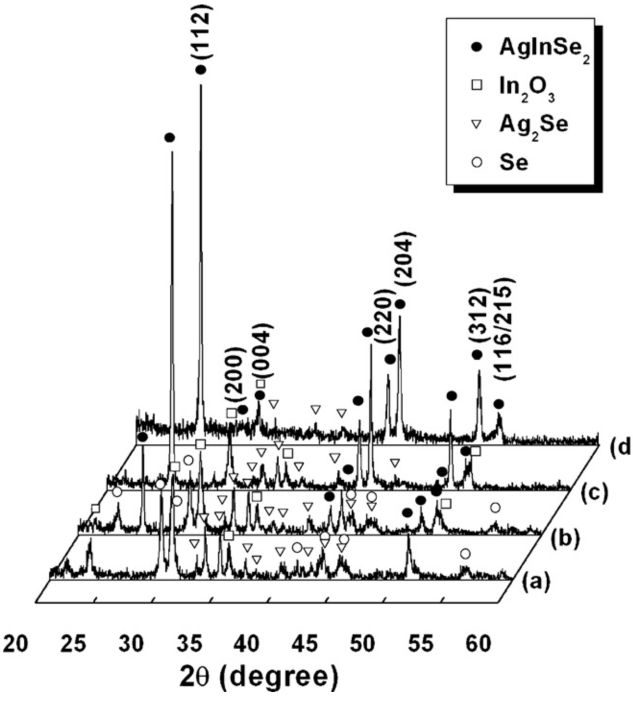

Fig. 8. X-ray diffraction patterns of $AgInSe_2$ precursors selenized at (a) 300 °C, (b) 400 °C, (c) 500 °C, and (d) 600 °C.

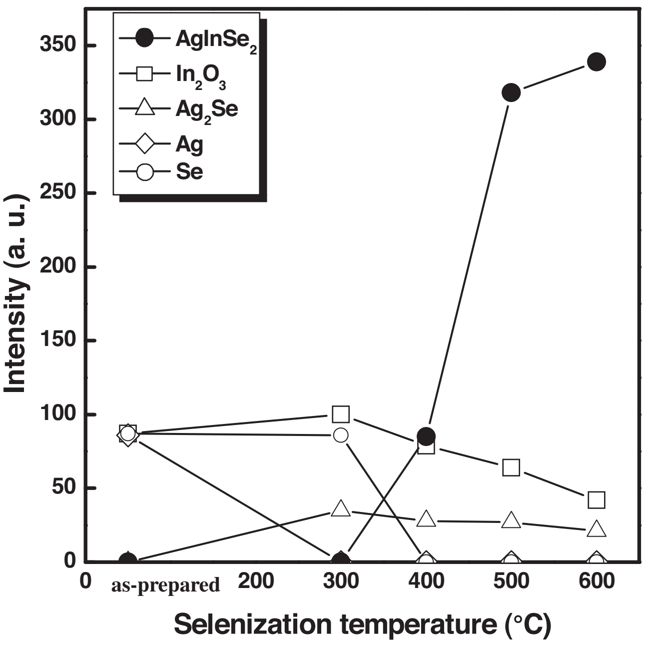

Fig. 9. Plot of diffraction peak intensities of the formed phases versus selenization temperatures.

$$2Ag + Se \xrightarrow{\sim 300\,^{\circ}C} Ag_2Se \qquad (1)$$

$$2In_2O_3 + 2Ag_2Se + 6Se \xrightarrow{400-600\,^{\circ}C} 4AgInSe_2 + 3O_2 \qquad (2)$$

The reaction process consists of two steps. In the first step, Ag reacts with Se to form Ag_2Se around 300 °C. When selenizing around 400 °C, Ag_2Se obtained in the first-step reaction starts to react with In_2O_3 and Se vapor to produce $AgInSe_2$ in the second-step reaction. Fig. 9 indicates that the amount of $AgInSe_2$ increases with a decrease in the amounts of Ag_2Se and In_2O_3 at 400–600 °C. This observation confirms the expressed reactions. The above result reveals that Ag_2Se is the intermediate compounds and initiates the formation reaction for $AgInSe_2$. Based on the proposed mechanism, increasing the reactivity of Ag_2Se with In_2O_3 and Se can improve the purity of the obtained $AgInSe_2$.

4. Conclusions

$AgInSe_2$ particles were successfully prepared via selenizing mixtures of sol–gel derived precursors and Se powders. It was discovered that excess amounts of In^{3+} ions were necessary in the sol–gel process to obtain the pure $AgInSe_2$ compound due to the lost of In_2O_3. The relation between the selenization conditions and resultant compounds can be depicted as a figure with four distinct zones. The pure $AgInSe_2$ phase was obtained at 450 °C for 2 h or at 600 °C for 20 min. The synthesized $AgInSe_2$ powders belonged to the chalcopyrite structure, which was confirmed via Raman analysis and X-ray diffraction analysis. The particle sizes and the crystallinity of the $AgInSe_2$ powders increased with increasing the selenization temperature. The reaction mechanism is proposed as a two-step reaction. Ag_2Se is formed in the first step and then leads to the $AgInSe_2$ formation reaction in the second-step. The sol–gel method with a selenization process was demonstrated to provide a potential approach to fabricate $AgInSe_2$ materials.

Acknowledgement

The authors would like to thank DuPont Taiwan Limited and the National Science Council, Taiwan, the Republic of China, for partial financial support of this study under Contract No. NSC 100-311-E-002-011.

References

[1] M.A. Green, Sol. Energy 76 (2004) 3.
[2] F.Y. Liu, C. Huang, Y.Q. Lai, Z. Zhang, J. Li, Y.X. Liu, J. Alloys Compd. 509 (2011) L129.
[3] C.H. Lu, C.H. Lee, C.H. Wu, Sol. Energy Mater. Sol. Cells 94 (2010) 1622.
[4] C.H. Lee, C.H. Wu, C.H. Lu, J. Am. Ceram. Soc. 93 (2010) 1879.
[5] M.C.S. Kumar, B. Pradeep, J. Alloys Compd. 495 (2010) 284.
[6] E. Lee, J.W. Cho, J. Kim, J. Yun, J.H. Kim, B.K. Min, J. Alloys Compd. 506 (2010) 969.
[7] P.P. Hankare, K.C. Rathod, P.A. Chate, A.V. Jadhav, I.S. Mulla, J. Alloys Compd. 500 (2010) 78.
[8] T. Yamaguchi, Y. Asai, N. Oku, S. Niiyama, T. Imanishi, S. Nakamura, Sol. Energy Mater. Sol. Cells 95 (2011) 274.
[9] S. Jun, S. Ahn, J.H. Yun, J. Gwak, D. Kim, K. Yoon, Curr. Appl. Phys. 10 (2010) 990.
[10] H. Karaagac, M. Kaleli, M. Parlak, J. Phys. D – Appl. Phys. 42 (2009).
[11] J.H. Shi, Z.Q. Li, D.W. Zhang, Q.Q. Liu, Z. Sun, S.M. Huang, Prog. Photovolt. Res. Appl. 19 (2011) 160.
[12] D. Pathak, R.K. Bedi, A. Kaushal, D. Kaur, Int. J. Mod. Phys. B 27 (2010) 5379.
[13] E. Lee, J.W. Cho, J. Kim, J. Kim, J. Yun, J.H. Kim, B.K. Min, J. Alloys Compd. 506 (2010) 969.
[14] T. Todorov, D.B. Mitzi, Eur. J. Inorg. Chem. (2010) 17.
[15] G.E. Delgado, A.J. Mora, Chalco. Lett. 6 (2009) 635–639.
[16] Y. Jin, K. Tang, C. An, L. Huang, J. Cryst. Growth 253 (2003) 429.
[17] L. Tian, M.T. Ng, N. Venkatram, W. Ji, J.J. Vittal, Cryst. Growth Des. 10 (2010) 1237.
[18] C.H. Hsu, C.L. Liaw, C.H. Lu, J. Alloys Compd. 489 (2010) 445.
[19] J. Liu, W. Zhang, C. Guo, Y. Zeng, J. Alloys Compd. 497 (2009) 863.
[20] H. Schoeller, J. Cho, J. Mater. Res. 24 (2009) 386.
[21] S.J. Ahn, C.W. Kin, J.H. Yun, J. Gwak, S. Jeong, B.H. Ryu, K.H. Yoon, J. Phys. Chem. C 114 (2010) 8108.
[22] L.S. Lerner, J. Phys. Chem. Solids 27 (l) (1966).
[23] J.L. Shay, B. Tell, H.M. Kasper, L.M. Shiavone, Phys. Rev. B 7 (1973).
[24] F.W. Ohrendorf, H. Haeuseler, Cryst. Res. Technol. 34 (1999) 339.